nature communications

Article

https://doi.org/10.1038/s41467-024-52262-0

Integrated landscape of plasma metabolism and proteome of patients with post-traumatic deep vein thrombosis

Received: 14 July 2023

Accepted: 2 September 2024

Published online: 07 September 2024

Check for updates

Kun Zhang[1,2,3,5], Pengfei Wang[1,5], Wei Huang[1,2,3,5], Shi-Hao Tang[2,3], Hanzhong Xue[1], Hao Wu[2,3], Ying Zhang[4], Yu Rong[2,3], Shan-Shan Dong[2,3], Jia-Bin Chen[1], Yan Zou[2,3], Ding Tian[1], Na Yang[1], Yifan Liang[1], Chungui Liu[1], Dongyang Li[1], Kun Zhang[1] ✉, Tie-Lin Yang[2,3] ✉ & Yan Guo[1,2,3] ✉

Deep vein thrombosis (DVT) is a leading cause of morbidity and mortality after trauma. Here, we integrate plasma metabolomics and proteomics to evaluate the metabolic alterations and their function in up to 680 individuals with and without DVT after trauma (pt-DVT). We identify 28 metabolites and 2 clinical parameter clusters associated with pt-DVT. Then, we develop a panel of 9 metabolites (hexadecanedioic acid, pyruvic acid, L-Carnitine, serotonin, PE(P-18:1(11Z)/18:2(9Z,12Z)), 3-Hydroxycapric acid, 5,6-DHET, 3-Methoxybenzenepropanoic acid and pentanenitrile) that can predict pt-DVT with high performance, which can be verified in an independent cohort. Furthermore, the integration analysis of metabolomics and proteomics data indicates that the upregulation of glycolysis/gluconeogenesis-TCA cycle may promote thrombosis by regulating ROS levels in red blood cells, suggesting that interfering with this process might be potential therapeutic strategies for pt-DVT. Together, our study comprehensively delineates the metabolic and hematological dysregulations for pt-DVT, and provides potential biomarkers for early detection.

Deep vein thrombosis (DVT) is a major health problem that can lead to a variety of complications, such as post-thrombotic syndrome, recurrent DVT, and life-threatening pulmonary embolism (PE)[1,2]. DVT and PE are collectively known as venous thromboembolism (VTE). Previous studies have identified multiple risk factors of DVT, such as advanced age, immobility, surgery, and hospitalization[1,3]. Particularly, the risk of DVT increased in trauma individuals secondary to injury patterns and immobility[3,4]. Post-traumatic DVT (pt-DVT) has long been recognized as one of the most relevant clinical problems in the adult population[5] since failure to recognize this common morbidity could lead to an unacceptable rate of PE. It is also a leading cause of morbidity and mortality after trauma[6,7]. Furthermore, traumatic bone fractures are a major public health issue in China[8], and the incidence of pt-DVT can reach up to 40%[9–12], which makes pt-DVT a serious threat to public health in China.

Currently, the diagnosis and treatment of pt-DVT follow the VTE management approach. The diagnosis relies on laboratory measures of D-dimer and specific imaging features of ultrasound (US)[1,13–15], while the treatment and prevention include widespread employment of anticoagulants, mechanical prophylaxis, or inferior vena cava filter (IVCF) placement[16]. Although D-dimer has been validated as a risk tool in hospitalized adult patients, the application in patients at risk of DVT

[1]Department of Trauma Surgery, Honghui Hospital, Xi'an Jiaotong University, Xi'an, Shaanxi, P. R. China. [2]Key Laboratory of Biomedical Information Engineering of Ministry of Education, Biomedical Informatics & Genomics Center, School of Life Science and Technology, Xi'an Jiaotong University, Xi'an, Shaanxi, P. R. China. [3]Key Laboratory of Biology Multiomics and Diseases in Shaanxi Province Higher Education Institutions, Xi'an Jiaotong University, Xi'an, Shaanxi, P. R. China. [4]Instrument Analysis Center, Xi'an Jiaotong University, Xi'an, Shaanxi, P. R. China. [5]These authors contributed equally: Kun Zhang, Pengfei Wang, Wei Huang. ✉e-mail: hhyyzk@126.com; yangtielin@xjtu.edu.cn; guoyan253@xjtu.edu.cn

after surgery or a traumatic event is unclear. In addition, surgery may cause secondary trauma, and prevention and early diagnosis of thrombosis in trauma patients are challenging during hospitalization and perioperative nursing. Therefore, the identification of biomarkers for pt-DVT is necessary and important to make an early diagnosis and provide appropriate DVT management.

Metabolomics is a promising approach for biomarker discovery, which could provide insights into pathology, treatment, and early diagnosis of diseases[17–19]. Although previous studies[20–22] have found several metabolic alterations associated with VTE, including carnitines, carnitine species, glucose, phenylalanine, 3-hydroxybutarate, lactic acid, tryptophan, and some monounsaturated and polyunsaturated fatty acids, our understanding on the global metabolic alterations in pt-DVT is still limited.

Therefore, to investigate the potential metabolic mechanisms of pt-DVT and recognize DVT patients among individuals with traumatic fractures, we used untargeted metabolomics with liquid chromatography-mass spectrometry (LC-MS) to systematically characterize plasma metabolites profiles between pt-DVT patients and controls and screened the hematological alterations associated with pt-DVT. Our study identified multiple metabolites, clinical parameters (CPs), and metabolic pathways for pt-DVT. Leveraging the multidimensional datasets, we further developed a panel of biomarkers using a machine learning method to discriminate post-traumatic DVT patients. It will be valuable for the design of an early diagnostic test for pt-DVT. Finally, by proteomics and metabolomics integrative analysis, we get insight into the altered metabolic pathways and provide potential therapeutic strategies for pt-DVT.

Results

Clinical characteristics of the studied cohort

The study design and analysis workflow is illustrated in Fig. 1. Based on the strict inclusion/exclusion criteria, a total of 680 patients were enrolled in the discovery ($N = 580$) and the validation ($N = 100$) cohorts. Briefly, for the discovery cohort, 252 patients diagnosed with incident pt-DVT were selected as cases, and 328 patients without DVT were selected as controls, which were enrolled from October 2018 to December 2020. Subsequently, from March 2021 to July 2021, 50 pt-DVT patients and 50 controls were selected with the same recruitment criteria as a separate validation cohort. The clinical characteristics of all the participants are shown in Supplementary Data 1, including 4 basic characteristics and 34 cardiovascular and hematological characteristics. The basic characteristics were approximately balanced between the pt-DVT group and controls.

Global plasma metabolic profiles

After MS/MS identification and data filtering, 326 metabolites that could be reproducibly detected in all batches were considered stable and reserved for subsequent analyses (Supplementary Data 2 and Supplementary Data 3). The identified metabolites were categorized into 8 functional groups and an unknown set according to the metabolism pathways in the Kyoto Encyclopedia of Genes and Genomes (KEGG) (Fig. 2a), including lipid, amino acid, xenobiotics, carbohydrate, nucleotide, peptide, cofactors, and vitamins, energy, and others. Principal components analysis (PCA) was performed to evaluate the global metabolic variations and data quality in metabolic analysis. The optimal separation of groups was obtained in PC 1 and 2, which accounted for 8.6% and 4.7% of the whole variance of the dataset, respectively (Supplementary Fig. 1).

Metabolite groups altered in pt-DVT

The volcano plot visualizes the significantly increased/decreased metabolites between the two groups by the univariate analysis (Fig. 2b). For multivariate analysis, we implemented orthogonal partial least squares discriminant analysis (OPLS-DA) (Fig. 2c) and identified 96 metabolites with a significant contribution to the variation (Fig. 2d). The permutation test was performed to evaluate the validity of the discriminant model to avoid overfitting (Supplementary Fig. 2). Together, a total of 28 metabolites (Supplementary Data 4) identified both by univariate and multivariate analyses were considered as significantly changed metabolites, including 11 lipids, 5 amino acids, 3 carbohydrates, 2 peptides, 2 nucleotides, 2 xenobiotics, 1 energy metabolic group, and 2 other groups. All 28 metabolites were used for hierarchical clustering in a heatmap separating the 2 groups (pt-DVT or Controls; Fig. 2e).

The debiased sparse partial correlation (DSPC) network (Fig. 3a) shows the relationships in which the partial correlation coefficients were significant (Supplementary Data 5). The topology of the network demonstrates dense interactions occurred between both inter- and intra-functional metabolite groups with the densest interactions between lipid and amino acid metabolism. Besides, metabolites of unknown function mainly occupied the position near these two metabolite groups, N2,N2-Dimethylguanosine, and pyruvic acid, suggesting that they may be involved in lipid, amino acid, nucleotide, and carbohydrate metabolism. Together, these findings indicate that a highly coordinated metabolite regulatory network underlies thrombosis.

Dysregulation of multiple metabolic pathways related to pt-DVT

For pathway analysis, a total of 307 metabolites could be mapped to 52 KEGG pathways. We identified 17 significantly dysregulated pathways involved in amino acid metabolism, carbohydrate metabolism, and lipid metabolism (Fig. 3b and Supplementary Data 6), suggesting a large-scale metabolic dysregulation in the pt-DVT group. The differential abundance (DA) score of 17 significantly altered pathways (Fig. 3c and Supplementary Data 6) showed that 6 pathways involved in amino acid metabolism were elevated activities. The activities of all 5 pathways associated with carbohydrate metabolism were notably upregulated, including the well-studied citrate cycle (TCA cycle) and glycolysis/gluconeogenesis. While the activities of all the 3 pathways associated with lipid metabolism were downgraded. Moreover, we identified several pathways for amino acid metabolism which were less studied with pt-DVT, such as Cysteine and methionine metabolism, Glycine, serine and threonine metabolism, Arginine and proline metabolism, Alanine, aspartate, and glutamate metabolism, and Histidine metabolism.

CP Clusters altered in pt-DVT

We identified 14 significantly changed CPs, 5 of which were increased in pt-DVT patients, and the others were decreased (Fig. 4a and Supplementary Data 7). The Pearson correlation analysis showed that the CPs were significantly increased/decreased and tended to cluster together (Fig. 4b). Interestingly, the clinical features with functional similarity were grouped within a cluster, such as the top increased CP cluster, including fibrinogen (Fbg), platelet hematocrit (PCT), and platelet count (PLT), while the most decreased cluster included the number of red blood cell count (RBC), hematocrit percentage (HCT), and hemoglobin concentration (HGB). Based on these, we revealed two typical clinical features for pt-DVT, one is increased PLT-PCT-Fbg cluster (named PLT cluster), and another one is decreased RBC-HCT-HGB cluster (named RBC cluster).

We further evaluated the diagnosis effects of these 6 CPs in PLT and RBC clusters for the diagnosis of pt-DVT (Supplementary Data 8). The results showed that PLT and PCT had excellent specificity for pt-DVT (Discovery cohort, PLT: specificity = 0.991; PCT: specificity = 0.994, Validation cohort, PLT: specificity = 0.96; PCT: specificity = 1) and might be the promising diagnostic markers for clinical use.

https://doi.org/10.1038/s41467-024-52262-0

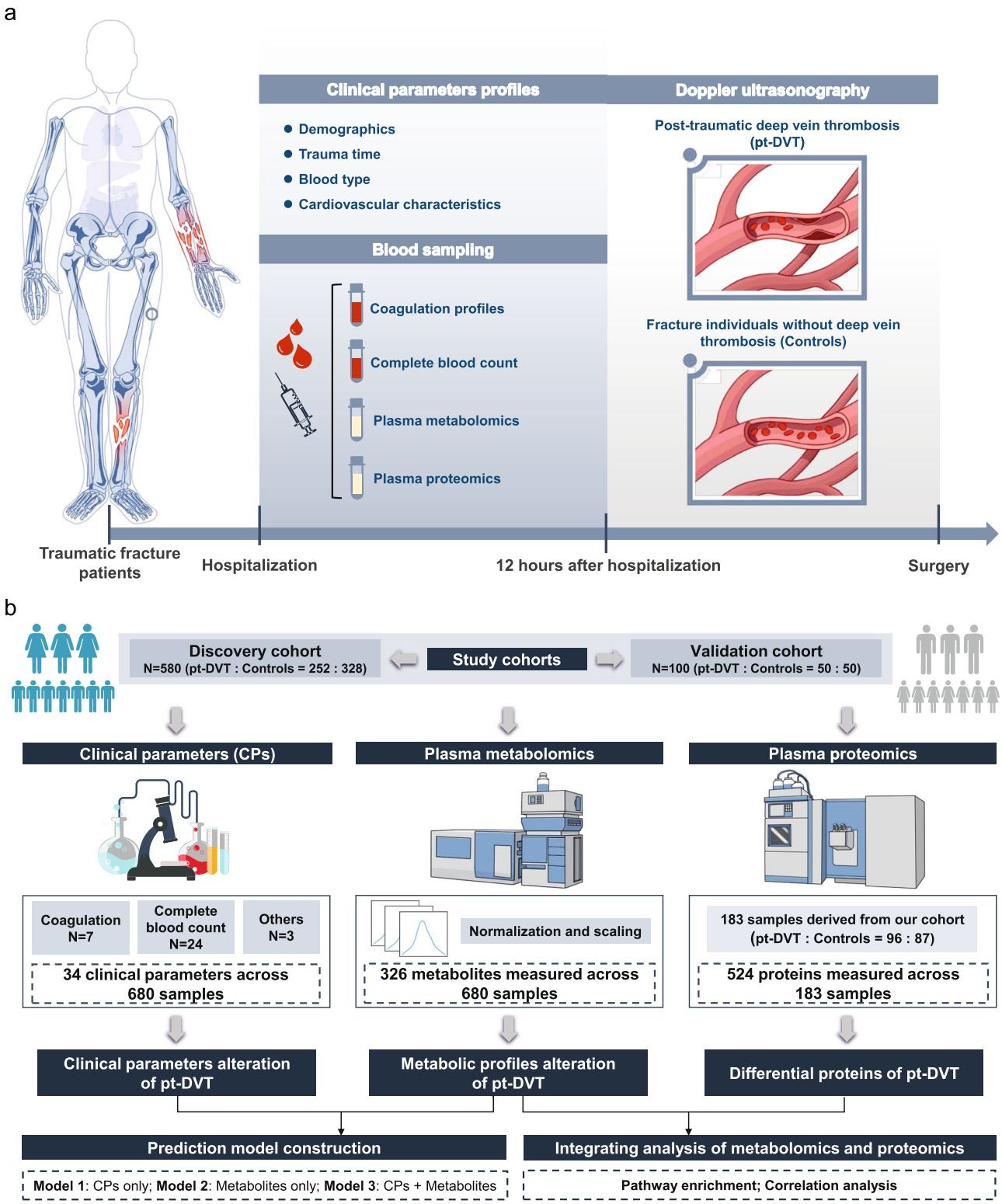

Fig. 1 | The design and analyses workflow of study. a The design of the current study. **b** The analysis workflow of the current study. OPLS-DA, orthogonal partial least squares discriminant analysis; DSPC, debiased sparse partial correlation; ROC, receiver operating characteristic.

Association between metabolic alteration and pt-DVT-related blood characteristics

The correlation matrix by Pearson coefficient presents the distinctive metabolic patterns for the PLT and RBC cluster (Supplementary Fig. 3). In total, 25 metabolites showed significant correlations with at least one of 6 CPs, of which 18 metabolites were related to the PLT cluster, while 17 metabolites were associated with the RBC cluster, indicating that the CPs within a cluster had similar metabolic patterns.

Next, using the linear regression model, we found 16 metabolites significantly associated with the PLT cluster (Fig. 4c and Supplementary Data 9) and 15 metabolites associated with the RBC cluster (Fig. 4d and Supplementary Data 9). We further conducted pathway-based quantitative enrichment using the metabolites associated with two

https://doi.org/10.1038/s41467-024-52262-0

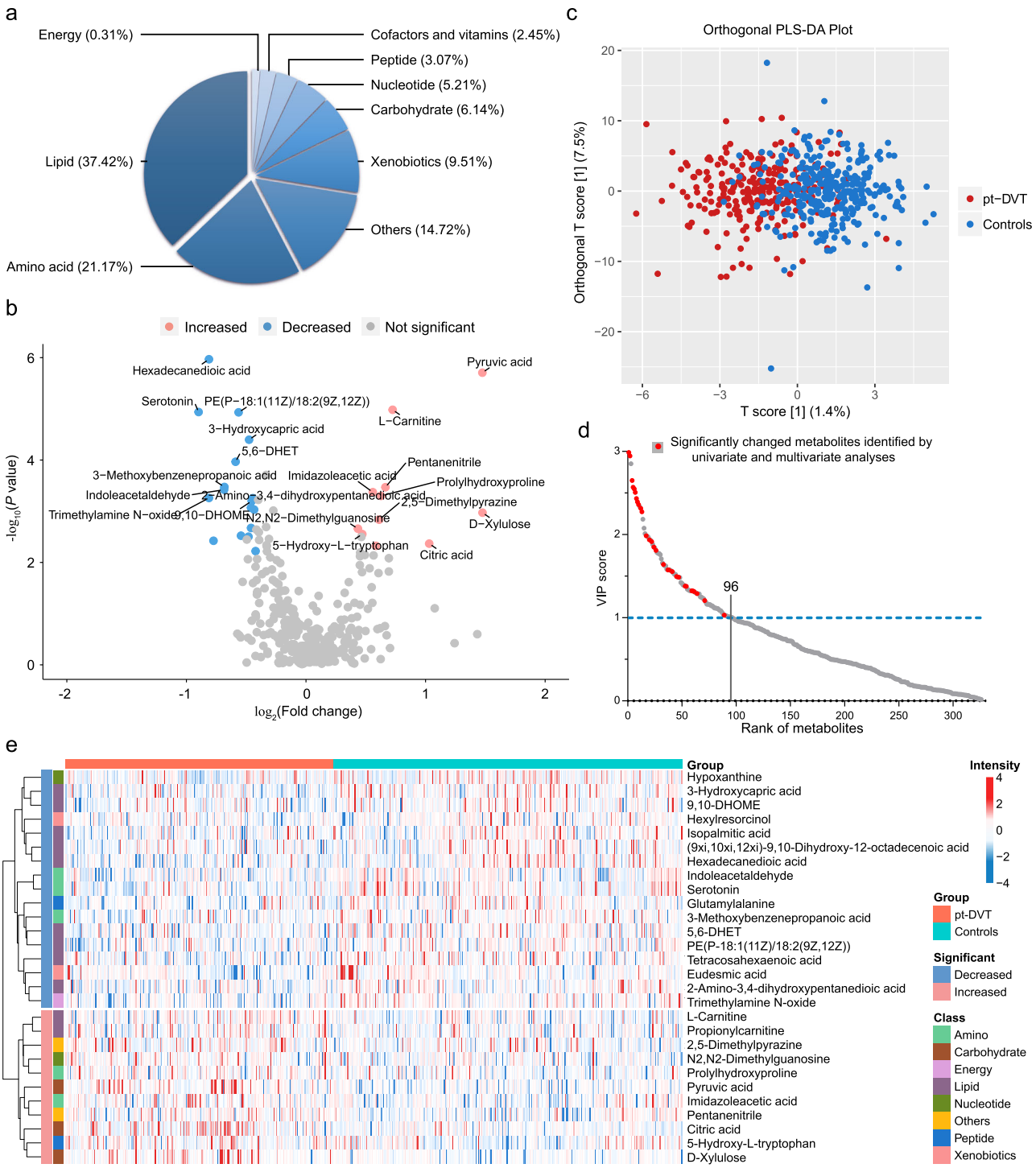

Fig. 2 | Metabolic profiles discriminating pt-DVT patients and controls. **a** Metabolite distribution over pathway-based classes. **b** Volcano plot of differential metabolites. The Benjamin-Hochberg false discovery rate (FDR) method was used to address multiple comparisons. Metabolites with a fold change of < 3/4 or > 4/3 and adjusted *P* value of two-tailed unpaired Student's *t* test/Mann-Whitney U-test less than 0.05 (FDR < 0.05) are considered significantly decreased (blue) or increased (pink). Changes in other metabolites are not significant. The top 10 increased and decreased metabolites are labeled. **c** Plot of orthogonal partial least squares discriminant analysis (OPLS-DA) score. **d** Variable importance in projection (VIP) score of OPLS-DA model. Red dots represent the metabolites that significantly (based on fold change and two-tailed unpaired Student's *t* test/Mann-Whitney U-test) altered in pt-DVT patients. **e** Heatmap of 28 differential metabolites throughout individuals. Red indicates metabolites that are increased, and blue indicates metabolites that are decreased in pt-DVT patients compared to controls. Source data are provided as a Source Data file.

clusters, respectively (Supplementary Data 10). As shown in Fig. 4e, 8 metabolic pathways that may regulate the alteration of the PLT cluster are mainly involved in lipid metabolism, especially with the oxidation of fatty acids. We identified 4 key metabolites in these pathways, including propionylcarnitine, l-carnitine, 5,6-DHET, and serotonin. Elevated plasma propionylcarnitine, l-carnitine, and serotonin levels were positively associated with PLT number, PCT, and Fbg level in the blood. Moreover, 26 metabolic pathways are related to the RBC cluster (Fig. 4f), including the pathways involved in amino acid metabolism, carbohydrate metabolism, and lipid metabolism. Apart from fatty acid

https://doi.org/10.1038/s41467-024-52262-0

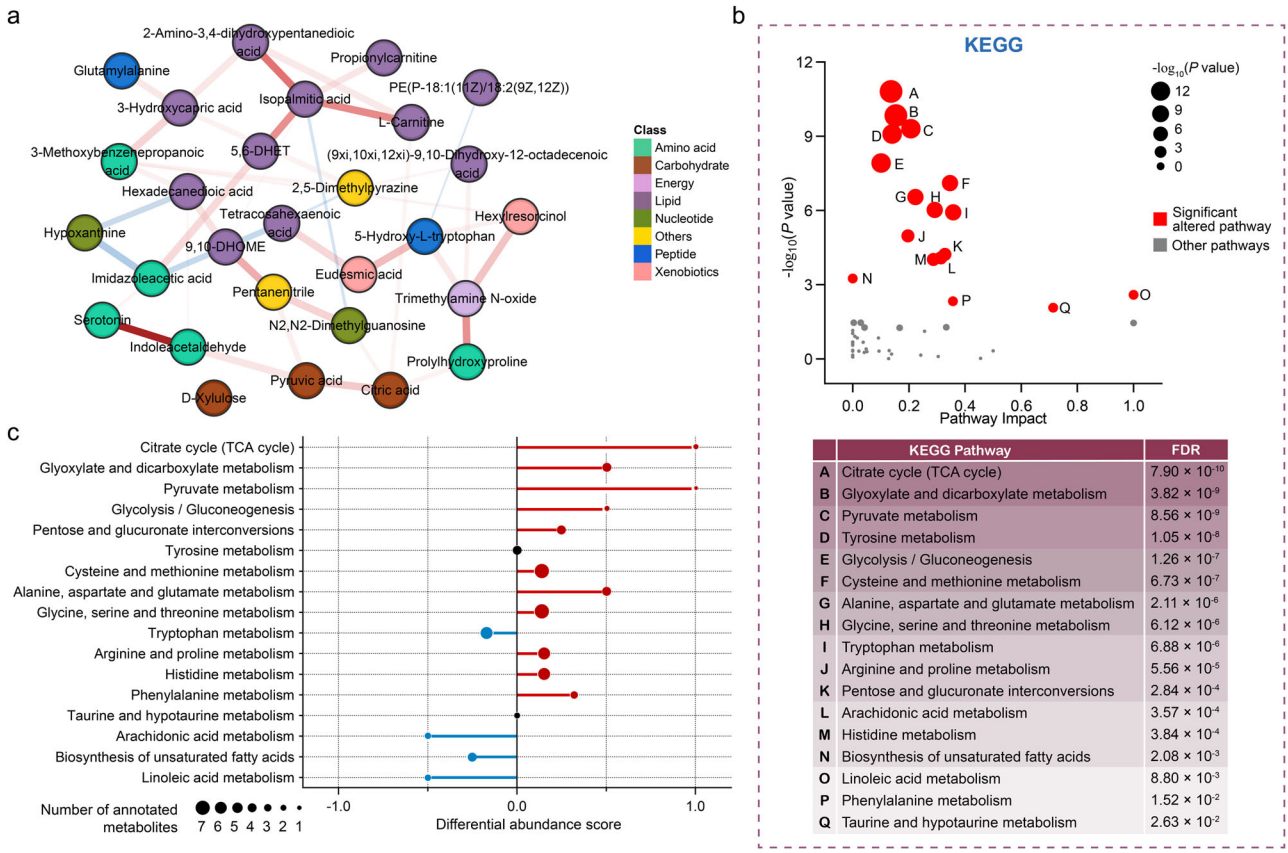

	KEGG Pathway	FDR
A	Citrate cycle (TCA cycle)	7.90×10^{-10}
B	Glyoxylate and dicarboxylate metabolism	3.82×10^{-9}
C	Pyruvate metabolism	8.56×10^{-9}
D	Tyrosine metabolism	1.05×10^{-8}
E	Glycolysis / Gluconeogenesis	1.26×10^{-7}
F	Cysteine and methionine metabolism	6.73×10^{-7}
G	Alanine, aspartate and glutamate metabolism	2.11×10^{-6}
H	Glycine, serine and threonine metabolism	6.12×10^{-6}
I	Tryptophan metabolism	6.88×10^{-6}
J	Arginine and proline metabolism	5.56×10^{-5}
K	Pentose and glucuronate interconversions	2.84×10^{-4}
L	Arachidonic acid metabolism	3.57×10^{-4}
M	Histidine metabolism	3.84×10^{-4}
N	Biosynthesis of unsaturated fatty acids	2.08×10^{-3}
O	Linoleic acid metabolism	8.80×10^{-3}
P	Phenylalanine metabolism	1.52×10^{-2}
Q	Taurine and hypotaurine metabolism	2.63×10^{-2}

Fig. 3 | Dysregulation of multiple metabolic pathways related to pt-DVT. **a** Debiased sparse partial correlation (DSPC) network of 28 significantly altered metabolites. Here, each node represents a metabolite, and each edge represents the strength of partial correlation between two metabolites. Edge weights represent the partial correlation coefficient. **b** Metabolic pathway undergoing significant changes in pt-DVT patients. The Benjamin-Hochberg false discovery rate (FDR) method was used to address multiple comparisons. Red dots mean pt-DVT related pathways with an adjusted *P* value of two-tailed Global test less than 0.05 (FDR < 0.05). **c** A pathway-based analysis of metabolic changes for pt-DVT. The differential abundance (DA) score captures the average gross change for all metabolite measures in a pathway. A score of 1 indicates that all annotated metabolites in the pathway increase in pt-DVT patients compared to controls, and a score of −1 indicates that all annotated metabolites in the pathway decrease. The size of the dot represents the number of annotated metabolites in the pathway. Source data are provided as a Source Data file.

oxidation and other pathways associated with lipid metabolism, increased imidazoleacetic acid and pyruvic acid levels were negatively associated with RBC number, HCT, and HGB levels in blood. It may contribute to pt-DVT pathogenesis through carbohydrate and amino acid metabolism, such as two additional energy metabolisms of the TCA cycle and glycolysis/gluconeogenesis.

Machine learning identified hematal-metabolic block to discriminate pt-DVT

To verify the generalization ability of the predictive model, we performed metabolomic analysis on 100 participants from an independent validation cohort (Supplementary Datas 11, 12). Firstly, we evaluated the performance of the three models using all significantly altered CPs ($N = 14$) and metabolites ($N = 28$) identified above and found that model 2 with 28 metabolites and model 3 with 42 predictors showed excellent predictability both in the discovery and validation cohort (Supplementary Fig. 4).

For potential clinical use, we next tested whether we could use fewer features to distinguish pt-DVT and choose *P* value ranking for model reduction due to better predictive performance (Supplementary Fig. 5a–c). Based on the results of model reduction, we, therefore, selected the top 9 predictors for each model. The prediction effects of the three models were rapidly reduced with the decreasing of features (Supplementary Fig. 5d–f). As shown in Fig. 5a, b, the performance of model 1 (Discovery cohort: AUC = 0.873, Validation cohort: AUC = 0.857), which predicted pt-DVT using only CPs was the worst, indicating that CPs alone might be not enough to diagnose pt-DVT at present. Correspondingly, model 2 (Discovery cohort: AUC = 0.956, Validation cohort: AUC = 0.935) and model 3 (Discovery cohort: AUC = 0.935, Validation cohort: AUC = 0.910) were well able to discriminate DVT from trauma patients, which suggested that plasma metabolites had a great contribution to pt-DVT early diagnosis and prediction in clinical use. In particular, the performance of model 2 comprising 9 metabolites (hexadecanedioic acid, pyruvic acid, L-Carnitine, serotonin, PE(P−18:1(11Z)/18:2(9Z,12Z)), 3-Hydroxycapric acid, 5,6-DHET, 3-Methoxybenzenepropanoic acid and pentanenitrile) (Fig. 5c) was superior to other models both in the discovery cohort and the validation cohort, indicating a better predictability and generalization ability.

Metabolomics and proteomics analyses reveal potential therapeutic strategies for pt-DVT

Considering that proteomics can provide an insightful metabolic perspective by profiling the metabolic proteins and contribute to the understanding of pt-DVT metabolism, we performed a global proteomics study on 96 pt-DVT patients and 87 control participants derived from our cohort. In total, 524 plasma proteins were quantified (Supplementary Datas 13, 14), and 214 proteins were identified as differential between the two groups (FDR < 0.05 and FC < 3/4 or > 4/3), with 153 upregulated and 61 downregulated in patients with pt-DVT (Fig. 6a and

https://doi.org/10.1038/s41467-024-52262-0

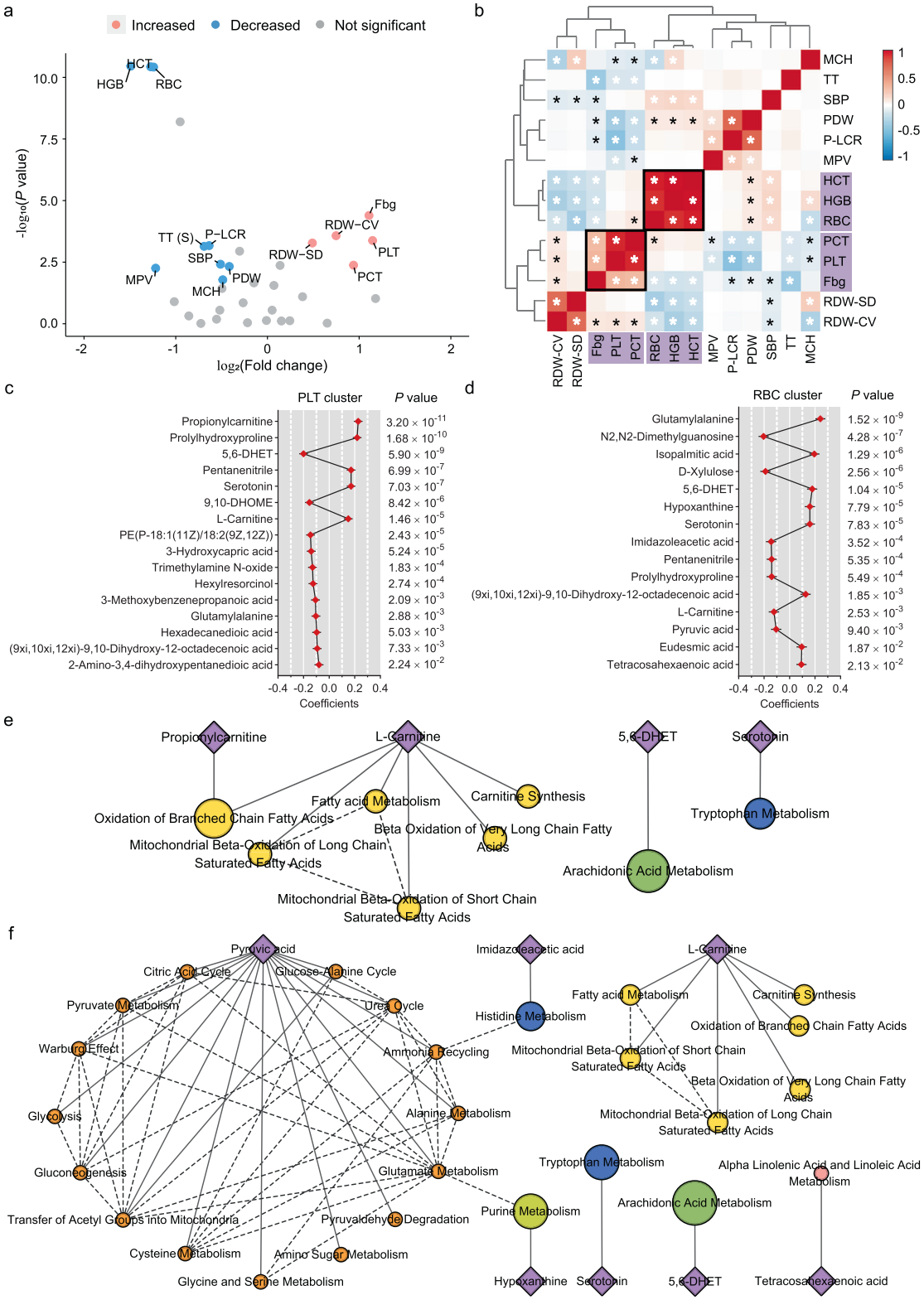

Supplementary Data 15). KEGG pathway enrichment of differential proteins found that 15 pathways were significantly altered (FDR < 0.05) in pt-DVT patients (Fig. 6b). Notably, complement and coagulation cascades were identified as the most significantly altered pathway, which is also the regulatory pathway that directly delivers to DVT.

Combining metabolomics and proteomics findings, we found that glycolysis/gluconeogenesis was changed both in metabolite and protein levels. Glycolysis/gluconeogenesis produces pyruvic acid for the TCA cycle, and our study revealed that pyruvic acid, citric acid, and several proteins in the glycolysis/gluconeogenesis pathway were significantly increased in pt-DVT patients. Therefore, it is reasonable to speculate that the upregulation of glycolysis/gluconeogenesis may result in the pathogenesis of thrombosis. This promoted us to further explore the roles of glycolysis/gluconeogenesis by integrating the metabolomics and proteomics data. As shown in Fig. 6c, we found 8 proteins (LDHA, LDHB, GAPDH, GPI, PKM, MINPP1, ENO1, and TPI1) upstream of pyruvic

https://doi.org/10.1038/s41467-024-52262-0

Fig. 4 | Differential clinical parameters for pt-DVT and related metabolic dysregulation. a Volcano plot of differential clinical parameters (CPs). The Benjamin-Hochberg false discovery rate (FDR) method was used to address multiple comparisons. CPs with a fold change of < 3/4 or > 4/3 and adjusted *P* value of two-tailed unpaired Student's *t* test/Mann-Whitney U-test less than 0.05 (FDR < 0.05) are considered significantly decreased (blue) or increased (pink). Changes in other CPs are not significant. All significant increased and decreased CPs are labeled. **b** Correlation matrix colored by the two-tailed Pearson correlation coefficient of each pair of pt-DVT-related CPs across samples. The Benjamin-Hochberg false discovery rate (FDR) method was used to address multiple comparisons. The asterisk (*) represents that each pair is significantly correlated (FDR < 0.05), and the *P* value < 0.0001 are marked in white. **c**, **d** Associations between pt-DVT related metabolites and PLT cluster (**c**) and RBC cluster (**d**) using linear regression model in 580 participants from the discovery cohort. The Benjamin-Hochberg false discovery rate (FDR) method was used to address multiple comparisons. Metabolites with adjusted two-tailed *P* value less than 0.05 (FDR < 0.05) are considered significant. Data are presented as coefficients ± SE. **e**, **f** Metabolic dysregulation associated with PLT cluster (**e**) and RBC cluster (**f**). Diamond represents the metabolite that was significantly (FDR < 0.05) associated with CP clusters, while ellipse is the pathway associated with the metabolites. Ellipse size represents the enrichment ratio of the pathway. Each edge represents that the metabolites can be annotated in the pathway, and the dotted edge suggests a close relationship between the pathways. Source data are provided as a Source Data file.

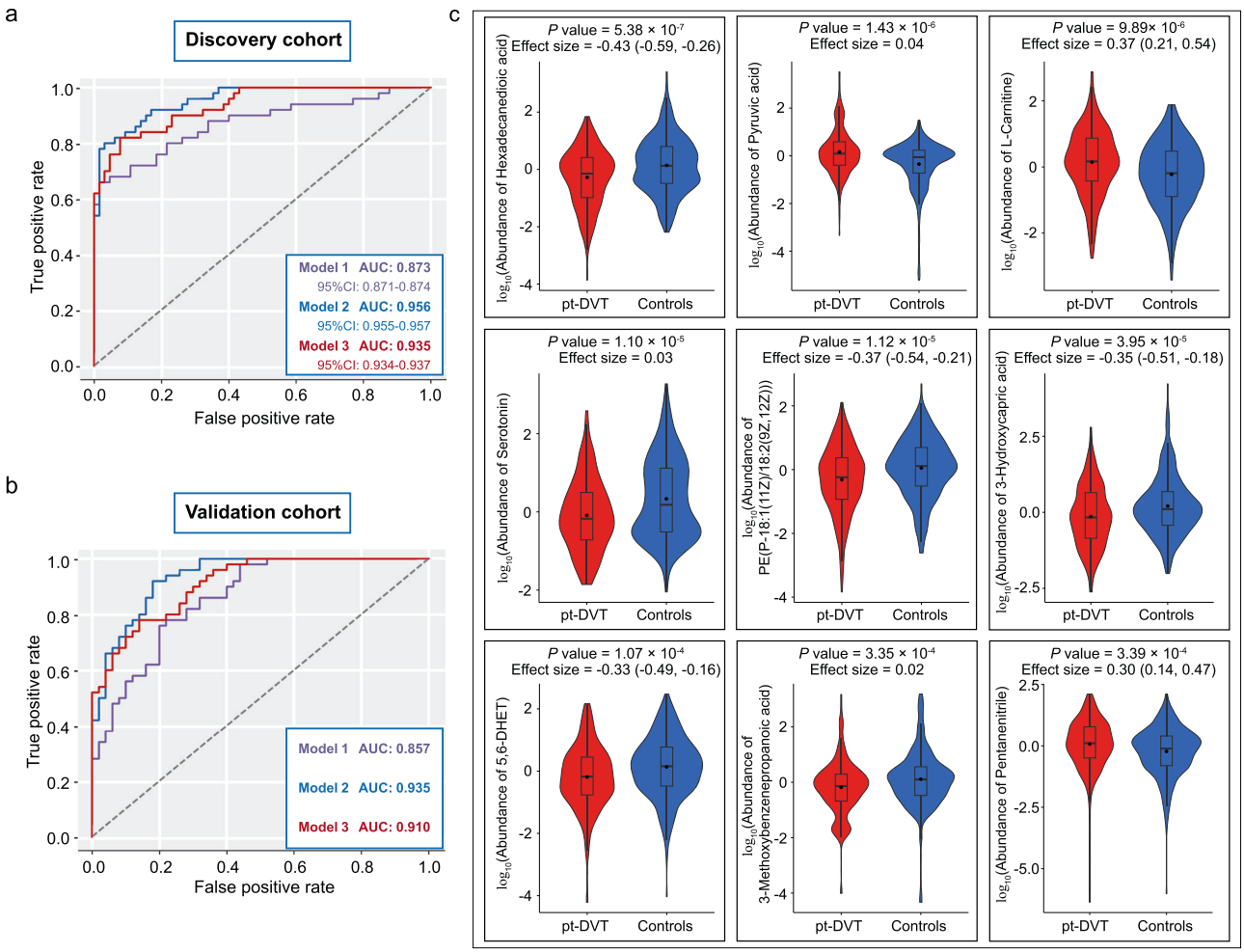

Fig. 5 | Machine learning identified features to discriminate pt-DVT. a Area under the receiver operating characteristic curve (AUROC) of model 1 (CPs only), model 2 (metabolites only), and model 3 (CPs and metabolites) in the discovery cohort. **b** AUROC of model 1, model 2, and model 3 in the validation cohort. **c** Box and violin plot shows the relative abundance of 9 features in model 2 across 580 samples in the discovery cohort. Statistical analyses were performed by two-tailed unpaired Student's *t* test/Mann-Whitney U-test, and data were presented as mean ± SD. The effect size of *t* test was presented as Cohen's D value and 95% confidence interval (CI). Box-plot, center line, median; box limits, upper and lower quartiles; whiskers, 1.5x interquartile range. Source data are provided as a Source Data file.

acid were significantly upregulated (FDR < 0.05, *P* value ranged from 2.88×10^{-10} to 1.87×10^{-2}) in pt-DVT patients. The glycolysis/gluconeogenesis-TCA cycle cascaded by pyruvic acid is a major source generating nicotinamide adenine dinucleotide (NADH), which plays a crucial role in the cellular redox status[23]. Previous studies have demonstrated that reactive oxygen species (ROS) in RBCs will alter erythrocyte membrane structure and be enhanced in thrombosis[24–26]. Consistent with these reports, our data indicated that ROS-related peroxiredoxins were slightly disturbed, with PRDX5 upregulated (FC = 1.558, *P* value = 2.71×10^{-2}) and PRDX2 downregulated (FC = 0.599, *P* value = 3.96×10^{-4}) in pt-DVT. The correlation analysis found that most differential proteins in the glycolysis/gluconeogenesis pathway (7/8) were significantly correlated with PRDX5 (Supplementary Fig. 6). In addition, lactate dehydrogenases (LDHA/LDHB), the most significantly changed proteins in glycolysis/gluconeogenesis, were reported to be involved in ROS production in a variety of cells[27,28]. It can be proposed that the upregulation of glycolysis/gluconeogenesis-TCA cycle cascaded by pyruvic acid may be associated with the accumulation of ROS in RBCs, thereby enhancing thrombosis. Together, our metabolomics and proteomics data highlight that intervening with glycolysis/gluconeogenesis

https://doi.org/10.1038/s41467-024-52262-0

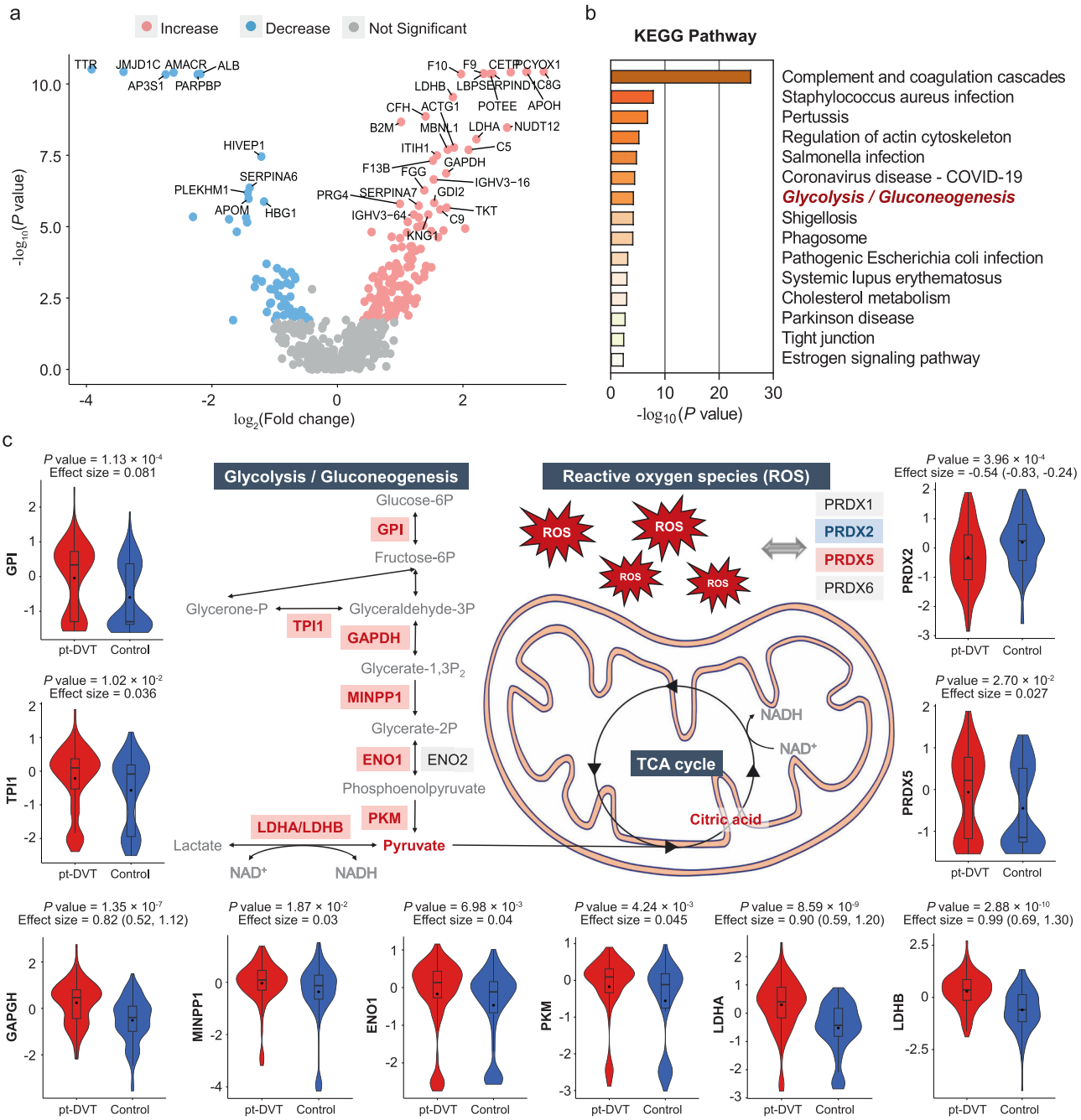

Fig. 6 | Metabolomics and proteomics analyses reveal potential therapeutic strategies for pt-DVT. a Volcano plot of differential proteins. The Benjamin-Hochberg false discovery rate (FDR) method was used to address multiple comparisons. Proteins with a fold change of < 3/4 or > 4/3 and adjusted *P* value of two-tailed unpaired Student's *t* test/Mann-Whitney U-test less than 0.05 (FDR < 0.05) are considered significantly decreased or increased. Changes in other proteins are not significant. The top 40 changed proteins are labeled. **b** KEGG pathway enrichment of differential proteins identified 15 significant pathways associated with pt-DVT. The Benjamin-Hochberg false discovery rate (FDR) method was used to address multiple comparisons. Pathways with an adjusted *P* value of one-tailed Fisher Exact test less than 0.05 (FDR < 0.05) are considered significant enrichment. **c** Schema of metabolic pathways (glycolysis/gluconeogenesis and TCA cycles) with select metabolites and proteins. Metabolites and proteins with upregulated, downregulated, and unchanged were colored in red, blue, and black, respectively. Gray nodes represent proteins that were not detected. Statistical analyses were performed by two-tailed unpaired Student's *t* test/Mann-Whitney U-test, and data were presented as mean ± SD. The effect size of *t* test was presented as Cohen's D value and 95% confidence interval (CI). Box-plot, center line, median; box limits, upper and lower quartiles; whiskers, 1.5x interquartile range. Source data are provided as a Source Data file.

and redox homeostasis might serve as potential therapeutic targets for pt-DVT. Based on these results, we performed pharmacological analysis with the related proteins associated with glycolysis/gluconeogenesis and redox homeostasis in our data and identified 50 potential compounds targeting glycolysis/gluconeogenesis and redox homeostasis (Supplementary Data 16), which facilitates subsequent functional studies and drug development.

Since inflammation appears to be central to the thrombosis[29–32], we also focused on the inflammation markers and found that C-reactive protein (CRP) was significantly elevated (*P* value = 2.39×10^{-4}) in the pt-DVT patients (Supplementary Data 15). To further assess the relationship between inflammation and pt-DVT-related metabolites and CPs, we performed linear regression in 156 participants, both measured proteomics and metabolomics. The results showed that CRP was

significantly associated with Fbg, RBC, HCT, HGB, and PE(P−18:1(11Z)/18:2(9Z,12Z)) (FDR < 0.05) (Supplementary Data 17), suggesting that the dysregulated lipid metabolism and hematological characteristics related to pt-DVT may be associated with the inflammatory response triggered after trauma.

Discussion

In two independent trauma cohorts, we identified a set of 28 metabolites and 14 CPs as potential biomarkers of pt-DVT, revealing the metabolic and hematological alterations in pt-DVT. Beyond that, we developed a panel of biomarkers including 9 features to distinguish pt-DVT patients efficiently using a machine learning algorithm, suggesting the potential clinical use of an early diagnostic test in pt-DVT. Finally, data resulting from integrative metabolomics and proteomic analyses indicated that the upregulation of glycolysis/gluconeogenesis-TCA cycle cascaded by pyruvic acid may be related to ROS in RBCs, thus enhancing thrombosis.

Based on our study design, the metabolites and pathways we identified may be potentially suggestive of DVT or involved in the mechanism of thrombosis. Among the changing metabolites and pathways, the major class that increased was carbohydrates, including pyruvic acid and citric acid, which participate in the TCA cycle and glycolysis. Pyruvic acid originated from pyruvate metabolism and glycolysis/gluconeogenesis is transported to the mitochondria where it is converted to acetyl coenzyme A (acetyl-CoA) and further produced as citric acid for the TCA cycle. The disturbance of the TCA cycle and glycolysis/gluconeogenesis have been reported to be closely related to venous thrombosis[20,33], but the role of pyruvate and citric acid in the disease remains unclear. Besides, another class that significantly changed in pt-DVT was lipids, particularly l-carnitine and fatty acids metabolism, which have been validated in previous studies[33–35]. It should be noted that some of the altered metabolites showed different trends in diverse studies due to discrepant detection platforms and study participants. For instance, Sung et al[33]. studied metabolic alterations in serum and vein wall extracts of the mouse model of DVT and found that citric acid was decreased in the DVT group, which was inconsistent with our finding. In contrast, l-carnitine was found to be of greater abundance in the serum of DVT animals[33], which was consistent with our study.

To get insight into the metabolic perspective and enhance the understanding of pt-DVT metabolism, we combined the proteomics data to profile the proteins related to pt-DVT metabolism. The integration of metabolomics and proteomics data suggested that the upregulation of pyruvic acid, citric acid, and several proteins in glycolysis/gluconeogenesis may produce more ROS and enhance thrombosis. ROS accumulate within RBCs due to endogenous hemoglobin autoxidation and uptake of extracellular ROS released by other cells. Previous studies[24,26] have found that elevated ROS in RBC affects the structure and function of RBC membranes, leading to loss of membrane integrity and reduced deformability. These alterations impair the function of RBCs in hemostasis and thrombosis by enhancing RBC aggregation, RBC binding to endothelial cells, RBC-induced platelet activation, RBC interaction with and activation of coagulation factors, and favoring a hypercoagulable state[24,26]. Consistent with these reports, ROS-related peroxiredoxins (PRDX5 and PRDX2) were also disturbed in our data. In addition, our study observed that lactate dehydrogenases (LDHA/LDHB) were drastically increased in pt-DVT, which have been reported to be involved in ROS production in a variety of cells[27,28]. A recent study[27] for cholangiocarcinoma found that LDHA and LDHB both exhibited hydrogen peroxide-producing activity or promoted oxidative stress in cancer cells in vitro and in vivo. Another study[28] in chondrocytes found that LDHA can promote ROS and may be a potential therapeutic target for osteoarthritis treatment. In general, our findings identified that intervening with glycolysis/gluconeogenesis and redox homeostasis might serve as potential therapeutic targets for pt-DVT in a relatively large population, while this hypothesis needs to be verified by further functional studies.

Among the changed CPs, we identified two major features, including the increased PLT-PCT-Fbg cluster and the decreased RBC-HGB-HCT cluster in pt-DVT patients. Accumulating evidence indicates that platelets contribute to thrombosis and might regulate effector functions of innate immune cells recruited to the thrombus[1,36]. Besides, mechanistic studies indicate that RBCs can promote thrombus formation and enhance thrombus stability[37]. When venous thrombosis is formed, a large number of RBCs will be recruited, which may result in a decrease in the number of RBCs in circulating blood. In addition to PLT and RBC, we also identified multiple pt-DVT-related CPs that have not been reported in previous studies, such as PCT, HGB, and HCT, of which PCT has the same excellent specificity for pt-DVT as PLT. It should be addressed that D-dimer (D-D), the laboratory measure for VTE or DVT diagnosis, did not significantly change in our study. Our data showed that D-D had the lowest false negative rates (FNR) (Supplementary Data 8), indicating that although D-D had poor specificity, it had the highest sensitivity and could be used as a preliminary indication for pt-DVT.

Assessment of the relationship between CPs and metabolites shows that the elevation of the PLT cluster is associated with lipid and amino acid metabolism, while the decrease of the RBC cluster is associated with energy metabolic processes, such as TCA cycle and glycolysis/gluconeogenesis, in addition to lipid and amino acid metabolism. The role of lipid metabolism, particularly fatty acids oxidation and arachidonic acid metabolism, in platelet promotion of thrombosis has not been well elucidated. A study[38] in diabetic patients found that l-carnitine might aggravate platelet hyperactivity by increasing the provision of surplus acetyl-CoA to the cytoplasmic compartment, which may explain the mediation of fatty acid oxidation in platelet promotion of thrombosis. In addition, l-carnitine has been shown to promote HGB elevation[39]. For RBC cluster-related metabolic dysregulation, the most interest is pyruvic acid involved in glycolysis/gluconeogenesis and TCA cycle, which was consistent with our findings that the upregulation of glycolysis/gluconeogenesis-TCA cycle cascaded by pyruvic acid may be associated with accumulation of ROS in RBCs, thus enhancing thrombosis.

It should be noted that the results that have been reported by other studies[20,22,33,40,41] mainly in patients without trauma, such as l-carnitine, pyruvic acid, citric acid, PLT, and RBC, which are not specific to post-traumatic DVT. Some of our findings that have not been reported might be specific to DVT after trauma, such as hexadecanedioic acid, D-Xylulose, 5,6-DHET, HGB, HCT, and PCT. However, the role of these metabolites and CPs in thrombosis for trauma patients is unclear. The traditional Virchow Triad pathogenetic mechanism of VTE indicates that venous injury, slow blood flow, and hypercoagulability of the blood are three important factors in thrombosis[1,42]. Trauma may trigger vascular injury and slow blood flow caused by immobility, leading to specific metabolic and hematologic features of DVT. For example, immobility in patients with bone fractures can disrupt venous flow in venous valves, thereby promoting platelet retention and contributing to thrombosis[43]. In addition, the inflammatory response triggered by vascular injury may also contribute to specific metabolic and hematologic patterns that favor thrombosis. Previous studies showed that CRP was not only a marker of inflammation but also had significant biological effects in regulating many of the aspects central to the pathogenesis of VTE[29]. The significant association results between CRP and Fbg, RBC cluster, and PE(P-18:1(11Z)/18:2(9Z,12Z)) suggest that the dysregulated lipid metabolism and hematological characteristics of pt-DVT may be related to the inflammatory response triggered by vascular injury. The detailed mechanisms of PE(P-18:1(11Z)/18:2(9Z,12Z)), RBC cluster, and Fbg in DVT are currently unknown, but observational studies have found that PE levels were prognostic for worse outcomes in trauma[32], while lipid

levels are associated with favorable changes in coagulation and inflammatory biomarkers in causal models[32]. Although there are no definitive studies elucidating how our findings play a role in the mechanism of inflammatory response-mediated thrombosis, observational studies have identified PE and lipids associated with trauma, inflammatory response, and coagulation, which may facilitate the traditional Virchow Triad pathogenetic mechanism of VTE.

An important result of this study is that we constructed a predictive model for pt-DVT using a machine learning algorithm. Using a similar approach, a recent study[22] identified plasma biomarkers to characterize venous thromboembolism. Nevertheless, the participants in the study were diagnosed with VTE rather than pt-DVT, and the plasma was collected 3 months after an incident VTE, which could not present the metabolic changes at disease states. Our design allowed us to sensitively capture the metabolic and hematological alterations in pt-DVT patients during thrombogenesis and to ensure good generalization ability of the prediction model through an independent cohort. We hypothesized that this information might help us to screen the more effective biomarkers and develop a more accurate diagnostic model to improve current trauma care through early diagnosis or prediction of thrombosis formation.

An apparent advantage of this study is the large sample size in pt-DVT metabolomics and proteomics analyses till now. This may give our study higher statistical power to guarantee reliable results. Meanwhile, the limitations of our study should also be addressed. First, due to the different medical treatment times, the trauma time before blood sampling in this study could not be unified. To eliminate this interference, we implemented multiple linear models fitted with 'sex', 'age', and 'time from trauma to sampling' as independent variables. Second, to obtain the metabolite that can be consistently detected for diagnostic biomarkers screening, we kept metabolites that were identified in all three batches for analysis, which may lead to the missing of some potentially relevant metabolites. Third, the severity of trauma is related to hemorrhage as such, the hematological alterations may be a surrogate for the severity of trauma, which could be associated with pt-DVT and thus confounding the results. Due to the lack of information on hemorrhage at the time of patient admission, we were unable to correct this problem during analyses. However, the participants in our study are only patients with mild trauma severity (ISS < 16) and with a similar trauma mode (trauma cause: 73.8% participants are falling during physical activity and biking; fracture location; 70.29% participants are femur, tibia or fibula), which may minimize the potential impact of trauma severity and hemorrhage. Fourth, our study is only suggestive of the metabolic changes and hematological characteristics associated with pt-DVT, and the in-depth mechanisms of thrombosis in trauma patients need more functional experiments to investigate.

In conclusion, this cohort study identified 28 metabolites and 14 CPs significantly associated with pt-DVT and comprehensively demonstrated the metabolic and hematological alterations in pt-DVT patients. Based on these significantly altered metabolites and CPs, we developed a panel of 9 metabolites to effectively distinguish pt-DVT patients. More importantly, combined with proteomics data, we found that the upregulation of the glycolysis/gluconeogenesis-TCA cycle cascaded by pyruvic acid may promote thrombosis regulating ROS levels in RBCs. It suggests that interfering with glycolysis/gluconeogenesis and redox homeostasis might be potential therapeutic strategies for pt-DVT treatment. In general, our study characterizes the metabolic dysregulation in pt-DVT and identifies plasma biomarkers with a large-scale cohort. We believe that our findings can facilitate functional research of pt-DVT, and contribute to early diagnosis for clinical use.

Methods

Ethics statement

The study was approved by the Ethics Committee of Xi'an Jiaotong University Honghui Hospital. All patients were provided written, informed consent before participating in the study. The study protocol can be available from the corresponding author upon reasonable request.

Study design and participants

The patients in our study were recruited as part of the study which was registered in the Chinese Clinical Trial Registry (ChiCTR) (Registration number: ChiCTR1800017754). It can be available in the World Health Organization (WHO) International Clinical Trials Registry Platform (ICTRP) (https://trialsearch.who.int/). The study design is illustrated in Fig. 1a. We carried out a nested case-control study design using a prospective cohort, which enrolled ~4000 Chinese Han participants diagnosed with acute traumatic fractures at the Department of Trauma Surgery, Honghui Hospital (Xi'an, China) from October 2018 to October 2022 (Fig. 1a). All participants were adult inpatients (over 18 years of age). All patients were not on anticoagulants or antiplatelet drugs before sampling, and fasting venous blood samples were obtained from each patient less than 12 hours after hospitalization. Follow-up assessments to determine DVT status were confirmed by US screening after blood sampling and prior to surgery, usually within 72 hours of admission. We didn't consider the sex of participants before the study design, and there were no sex-based analyses in our study because we corrected all data for sex as a covariate.

Based on this prospective cohort, we adopted strict inclusion/exclusion criteria to select samples for our study: (i) participants with major diseases or known metabolic diseases were excluded, including type 2 diabetes, coronary artery disease, hypertension, obesity, kidney or liver diseases, hyperthyroidism, dyslipidemia, and cancers; (ii) participants with chronic use of medications affecting metabolism (hormone replacement therapy and corticosteroid therapy) were excluded; (iii) we mainly focused on traumatic fractures (falling during physical activity and biking: 73.8%; traffic accident: 12.9%; falling down from a high altitude: 9.4%; and crushing by the heavy object: 3.9%), and participants with osteoporotic fractures or anti-osteoporosis drug intake were excluded to minimize potential influence on metabolic backgrounds; (iv) we focused on lower extremity fractures (femur: 50%; tibia or fibula: 20.29%; pelvis: 6.62%; knee: 9.85%; ankle: 6.03%; multiple bone fractures: 7.21%) and included only patients with mild trauma severity based on the Injury Severity Score (ISS) (definition of mild injury: ISS ≤ 16) to reduce the potential impact of trauma severity or mode; (v) all cases were patients with distal DVT of lower extremity (DVT involved the gastroc-soleal veins: 63.89%; DVT involved the axial calf veins: 10.32%; DVT involved both the axial calf veins and the gastroc-soleal veins: 25.79%) and the thrombi in all cases were relatively large in size (>10 millimeters × 2 millimeters, length × width). Based on the strict inclusion/exclusion criteria, 20.1% of patients were diagnosed as pt-DVT cases.

Clinical parameters characterization

The participants were required to fast overnight before blood collection and tested for three cardiovascular characteristics, including heart rate, systolic blood pressure (SBP), and diastolic blood pressure (DBP) in the meantime. Coagulation tests and complete blood count (CBC) were performed in the clinical laboratory of Honghui Hospital using the reagents purchased from SUNBIO (Shanghai, China) coupled with an Automatic Coagulation Analyzer (Sysmex, Japan) and an Automatic Hematology Analyzer (Sysmex, Japan).

Plasma metabolomics analysis

We performed untargeted metabolomics analyses on the discovery and validation cohorts, respectively. The discovery cohort was used to identify pt-DVT-related metabolic features and explore their relationships with CPs. Based on the identified metabolic and clinical features, we constructed a prediction model for pt-DVT using a machine learning algorithm. To further evaluate the generalization ability of the

model, we assessed the predictive performance of the corresponding metabolic and clinical features in the validation sample. All the plasma samples from both cohorts were separated from whole blood and extracted using chemical reagents for metabolomics analysis. Samples from the discovery cohort were analyzed in 2 batches at different time points, and the samples from the validation cohort were analyzed in a separate batch. The quality control (QC) sample was prepared by mixing an equal aliquot of the supernatants from all of the samples. We used the same QC (mixed in batch 1) for all batches. LC-MS/MS analyses were performed using a UHPLC system (Vanquish, Thermo Fisher Scientific) with a UPLC BEH Amide column (2.1 mm × 100 mm, 1.7 μm) coupled to Q Exactive HFX mass spectrometer (Orbitrap MS, Thermo). For each data batch, the acquisition order of all samples was randomly distributed and the QC injections were inserted every 10 samples injections. The raw data were converted to the mzXML format and processed with an in-house program, which was developed using R and based on XCMS[44]. Then, an in-house MS/MS database (BiotreeDB) was applied in metabolite annotation and the cutoff of similarity score was set at 0.4. The in-house software package and database have been widely used in many metabolic studies[45–48]. For the features detected in both positive and negative modes, we kept the one with a higher annotation score. Within a different analytical batch, all metabolic peaks were filtered to remove noise. After data filtering, the abundances of remaining peaks were normalized by dividing the intensity of internal standard (IS), and the data were log-transformed and scaled by median centered within a batch[17]. Metabolites measured in all batches were retained for study. Additional details about plasma metabolomics analysis are available in Supplementary Methods.

Plasma proteomics analysis

Sample preparation, including protein denaturation, reduction, alkylation, digestion, and peptide cleaning, was performed according to the iST kit (PreOmics, Germany) protocol. All samples were redissovled and added 11 tryptic iRT peptides (Biognosys, KI-3002-1) for LC-MS analysis. The peptide mixture was fractionated by high pH separation using the Ultimate 3000 system (ThermoFisher scientific, MA, USA) connected to a reverse phase column (XBridge C18 column, 4.6 mm × 250 mm, 5 μm, Waters Corporation, MA, USA). A total of 14 fractions were collected and analyzed by Q Exactive™ Plus coupled to a U3000 system (Thermo Fisher Scientific, MA, USA). The mass spectrometer was run under data-dependent acquisition (DDA) mode, and automatically switched between MS and MS/MS mode. Raw Data of DDA were processed and analyzed by Spectronaut 16.0 (Biognosys AG, Switzerland) with default settings to generate an initial target list. Furthermore, the mass spectrometer was run under data-independent acquisition (DIA) mode with a hybrid data strategy[49]. Raw Data of DIA were processed by Spectronaut 17.0 (Biognosys AG, Switzerland) software with default settings. The summation of the top 3 filtered peptides that passed the 1% false discovery rate (FDR) cutoff was used to calculate the major group quantities. Based on processed protein profiles, we also conducted data imputation consistent with metabolomics data. After data filtering, the abundances of remaining proteins were log-transformed and scaled by median centered. Additional details about plasma proteomics analysis are available in Supplementary Methods.

Statistical analyses

The Benjamin-Hochberg false discovery rate (FDR) method was used to address multiple comparisons issue, and the significance threshold of all statistical analyses in our study is corrected P value less than 0.05. All statistical analyses were performed using R software (version 3.6.1).

Covariate adjustment

The whole analyses workflow is illustrated in Fig. 1b. To minimize the influence of confounding factors, the metabolites, proteomics and clinical parameters profile data were first corrected with “sex”, “age”, and “trauma time” as covariates. In short, a multiple linear model was fitted with ‘sex’, ‘age’, and ‘trauma time’ as independent variables and the relative abundance of each metabolite, protein and CP as the dependent variable. The correction for metabolites and CPs was performed within the discovery and the validation cohorts separately. The correct data were residuals transformed and were scaled by median centered for subsequent analysis. After data pre-processing, we evaluated whether all metabolites, proteins, and CPs conformed to a normal distribution (P value > 0.05) using the Kolmogorov-Smirnov (KS) Test. The two-tailed Student’s t tests were performed for normally distributed features, and the two-tailed Mann-Whitney U-tests were used for non-normally distributed features. The effect size of the statistical test was calculated using the Computation of Effect Sizes (http://www.psychometrica.de/effect_size.html) website, with Cohen’s D value used for t test and Eta squared (η^2) used for the U-test.

Identification of differential metabolites for pt-DVT

Identification of significant alteration metabolites was performed using a two-step approach comprising univariate analysis and multivariate analysis in the discovery cohort. For univariate analysis, we performed a two-tailed unpaired Student’s t test/Mann-Whitney U-test and fold change (FC) to select differential metabolites. FDR < 0.05, and FC > 4/3 or < 3/4 was considered significant[18]. In multivariate analysis, unsupervised PCA was performed to explore the global metabolic variations between cases and controls. The supervised OPLS-DA[50] was used to maximize the global metabolic variations between two groups, and the metabolites with the threshold of variable importance in projection (VIP) score > 1 were supposed to significantly change. The OPLS-DA model was validated by 1000 permutation tests to avoid overfitting. The metabolites that up to all significant criteria were used for hierarchical clustering and DSPC network analysis (R package MetaboAnalystR)[51], which can capture the association between two metabolites after conditioning on all other variables in the network. The partial correlation coefficients were significant at FDR < 0.05, and the visualization of the DSPC network was realized by Cytoscape software[52].

Metabolic pathway analysis

The metabolic pathway analysis was performed with all identified metabolites utilizing MetaboAnalystR 5.0 (https://www.metaboanalyst.ca/MetaboAnalyst/home.xhtml)[53,54]. The metabolites were mapped into the KEGG database, and the statistical significance of the changes in a pathway’s activity between two groups was evaluated by global testing (FDR < 0.05). The topological pathway impacts were calculated according to relative-betweenness centrality. To quantify pathway activity, we calculated the DA score to demonstrate the tendency for a pathway with increased/decreased levels of metabolites compared to the control group[48]. The DA score was calculated by applying a differential abundance test (FDR corrected Student’s t tests) to all metabolites in a pathway. After determining which metabolites were significantly altered, the DA score was defined as:

DA score = (No. of metabolites increased -No. of metabolites decreased)/No. of measured metabolites in the pathway.

In short, the DA score varies from −1 to 1 which indicates all metabolites in a pathway decreased or increased in abundance.

Identification of differential CPs and the related metabolic characterization

For clinical profiling, we used logistic regression (R function glm), two-tailed unpaired Student’s t test/Mann-Whitney U-test, and FC to select significantly altered CPs in the discovery cohort. FDR < 0.05, and FC > 4/3 or < 3/4 was considered significant. To get insight into the metabolic dysregulation of pt-DVT-related blood characteristics above, Pearson correlation analysis was applied to evaluate the

association between a pair of CPs and pt-DVT-related metabolites. FDR < 0.05 was considered a significant correlation. In addition, a linear regression model was carried out to identify the metabolites associated with altered CP clusters (FDR < 0.05), which used the relative abundances of metabolites as the independent variables and the average level of CPs in a cluster as the dependent variables. The metabolites identified above were further employed to conduct pathway-based quantitative enrichment based on the small molecule pathway database (SMBPD)[55] using MetaboAnalystR 5.0[56].

Identification of differential proteins for pt-DVT and pharmacological evaluation

For proteomics data, we also used two-tailed unpaired Student's *t* test/Mann-Whitney U-test and FC to select significantly altered proteins associated with pt-DVT. FDR < 0.05, and FC > 4/3 or < 3/4 was considered significant. KEGG pathway analysis was performed with differential proteins using The Database for Annotation, Visualization, and Integrated Discovery (DAVID) website, and FDR < 0.05 was considered significantly enriched. For the potential target proteins screened in conjunction with metabolomics, we used the Connectivity Map (CMAP) (https://clue.io/)[57] to identify compounds with pt-DVT-related proteins[58]. Based on their algorithm, compounds with lower scores showed better overall inhibition of all input genes, and we show results with scores less than -99, considered as potential compounds for targeting pathways.

Machine learning for pt-DVT prediction

To predict pt-DVT from bone-fractured patients, we built the prediction models developed with support vector machine (SVM; R package e1071) algorithms. We tried three kernel parameters of the SVM algorithm (Linear, Radial Basis Function, Polynomial) and chose the best-performing polynomial for model construction. Based on different feature groups, we developed 3 models, including CPs only (model 1), metabolites only (model 2), and the full model comprising CPs and metabolites (model 3). The prediction ability was assessed by the area under the curve (AUC) of the receiver operating characteristic (ROC) curve (R package pROC). In addition, the bootstrap method was applied 1000 times in the discovery cohort to develop the training sets and the test sets (8:2) to dilute the selection bias. The discovery cohort was divided into training sets ($N = 465$, pt-DVT: controls = 202: 263) and test sets ($N = 115$, pt-DVT: controls = 50: 65) by bootstrap method, and the validation cohort ($N = 100$, pt-DVT: controls = 50: 50) was used to further evaluate the generalization ability of the model. We selected features by model reduction method according to the *P* value (*t* test/U-test, in all 580 samples from the discovery cohort) and the importance (SVM model, mean value of 1000 training sets) of potential variates. Then, the performance of the prediction model was evaluated in test sets and independent validation cohorts. Based on the bootstrap method, we obtained the AUC 1000 times in test sets and calculated the 95% confidence interval (95% CI). Besides, we chose the data division that corresponded to the average value of 1000 AUC as the final statistical model.

Reporting summary

Further information on research design is available in the Nature Portfolio Reporting Summary linked to this article.

Data availability

All relevant data support the key findings of this study are available within the article and its Supplementary Information files. Source data are provided in this paper. The raw intensity values and processed data matrix of metabolomics and proteomics are available in Supplementary Data. The mass spectrometry metabolomics data generated in this study have been deposited in the OMIX, China National Center for Bioinformation / Beijing Institute of Genomics, Chinese Academy of Sciences (https://ngdc.cncb.ac.cn/omix)[59,60] under accession code OMIX005819. The mass spectrometry proteomics data generated in this study have been deposited in the ProteomeXchange (https://proteomecentral.proteomexchange.org) Consortium via iProX repository[61,62] with the dataset identifier PXD054131. Raw data for clinical information are available from the corresponding author upon request. All data in this study is only allowed for academic use. Source data are provided in this paper.

Code availability

No custom code or mathematical algorithm was used in the methods. All statistical analyses were conducted in R using published libraries and functions.

References

1. Wolberg, A. S., et al. Venous thrombosis. *Nat. Rev. Dis. Primers* **1**, 15006 (2015).
2. Kafeza, M. et al. A systematic review of clinical prediction scores for deep vein thrombosis. *Phlebology* **32**, 516–531 (2017).
3. Beckman, M. G., Hooper, W. C., Critchley, S. E. & Ortel, T. L. Venous thromboembolism a public health concern. *Am. J. Prev. Med.* **38**, S495–S501 (2010).
4. Strandvik, G., El-Menyar, A., Asim, M., Galwankar, S. & Al-Thani, H. Clinical characteristics, management practices, and in-hospital outcomes among trauma patients with venous thromboembolism. *J. Emerg. Trauma Shock* **13**, 124–130 (2020).
5. Geerts, W. H., Code, K. I., Jay, R. M., Chen, E. L. & Szalai, J. P. A prospective-study of venous thromboembolism after major trauma. *N. Engl. J. Med.* **331**, 1601–1606 (1994).
6. Rogers, F. B. Venous thromboembolism in trauma patients: A review. *Surgery* **130**, 1–12 (2001).
7. Knudson, M. M., Gomez, D., Haas, B., Cohen, M. J. & Nathens, A. B. Three thousand seven hundred thirty-eight posttraumatic pulmonary emboli a new look at an old disease. *Ann. Surg.* **254**, 625–632 (2011).
8. Chen, W. et al. National incidence of traumatic fractures in China: a retrospective survey of 512 187 individuals. *Lancet Glob. Health* **5**, E807–E817 (2017).
9. Dwyer, K. M. et al. Predictors of posttraumatic deep vein thrombosis (DVT): Hospital practice versus patient factors-An analysis of the National Trauma Data Bank (NTDB) DISCUSSION. *J. Trauma* **66**, 999–1001 (2009).
10. Zhang, B. F. et al. Deep vein thrombosis in bilateral lower extremities after hip fracture: a retrospective study of 463 patients. *Clin. Inter. Aging* **13**, 681–689 (2018).
11. Zee, A. A. G., van Lieshout, K., van der Heide, M., Janssen, L. & Janzing, H. M. J. Low molecular weight heparin for prevention of venous thromboembolism in patients with lower-limb immobilization. *Cochrane. Db. Syst. Rev.* https://doi.org/10.1002/14651858.CD006681.pub4 (2017).
12. Cerbasi, S. et al. Assessment of deep vein thrombosis using routine pre- and postoperative duplex Doppler ultrasound in patients with pelvic trauma. *Bone Jt. J.* **104-B**, 283–289 (2022).
13. Palareti, G. et al. D-dimer testing to determine the duration of anticoagulation therapy. *N. Engl. J. Med.* **355**, 1780–1789 (2006).
14. Tritschler, T., Kraaijpoel, N., Le Gal, G. & Wells, P. S. Venous thromboembolism advances in diagnosis and treatment. *JAMA* **320**, 1583–1594 (2018).
15. Chopard, R., Albertsen, I. E. & Piazza, G. Diagnosis and treatment of lower extremity venous thromboembolism: A review. *JAMA* **324**, 1765–1776 (2020).
16. Toker, S., Hak, D. J. & Morgan, S. J. Deep vein thrombosis prophylaxis in trauma patients. *Thrombosis* **2011**, 505373–505373 (2011).
17. Liang, L. et al. Metabolic dynamics and prediction of gestational age and time to delivery in pregnant women. *Cell* **181**, 1680–1692 (2020).

18. Shen, X. et al. Serum metabolomics identifies dysregulated pathways and potential metabolic biomarkers for hyperuricemia and gout. *Arthritis Rheumatol.* **73**, 1738–1748 (2021).
19. Liu, J. et al. Integrative metabolomic characterisation identifies altered portal vein serum metabolome contributing to human hepatocellular carcinoma. *Gut* **71**, 1203–1213 (2022).
20. Franczyk, B., Gluba-Brzozka, A., Lawinski, J., Rysz-Gorzynska, M. & Rysz, J. Metabolomic Profile in Venous Thromboembolism (VTE). *Metabolites* **11**, 495 (2021).
21. Escobar, M. Q., et al. Serum metabolic profiles based on nuclear magnetic resonance spectroscopy among patients with deep vein thrombosis and healthy controls. *Metabolites* **11**, 874 (2021).
22. Fraser, K. et al. Plasma biomarkers and identification of resilient metabolic disruptions in patients with venous thromboembolism using a metabolic systems approach. *Arterioscler. Thromb. Vasc. Biol.* **40**, 2527–2538 (2020).
23. Chini, C. C. S., Zeidler, J. D., Kashyap, S., Warner, G. & Chini, E. N. Evolving concepts in NAD(+) metabolism. *Cell Metab.* **33**, 1076–1087 (2021).
24. Bettiol, A. et al. Erythrocyte oxidative stress and thrombosis. *Expert Rev. Mol. Med.* **24**, e31 (2022).
25. Lichota, A., Szewczyk, E. M. & Gwozdzinski, K. Factors affecting the formation and treatment of thrombosis by natural and synthetic compounds. *Int. J. Mol. Sci.* **21**, 7975 (2020).
26. Wang, Q. H. & Zennadi, R. Oxidative stress and thrombosis during aging: The roles of oxidative stress in RBCs in venous thrombosis. *Int. J. Mol. Sci.* **21**, 4259 (2020).
27. Wu, H. et al. Lactate dehydrogenases amplify reactive oxygen species in cancer cells in response to oxidative stimuli. *Signal Transduct. Tar.* **6**, 242 (2021).
28. Arra, M. et al. LDHA-mediated ROS generation in chondrocytes is a potential therapeutic target for osteoarthritis. *Nat. Commun.* **11**, 3427 (2020).
29. Dix, C. et al. C-reactive protein, immunothrombosis and venous thromboembolism. *Front. Immunol.* **13**, 1002652 (2022).
30. Branchford, B. R. & Carpenter, S. L. The role of inflammation in venous thromboembolism. *Front. Pediatr.* **6**, 142 (2018).
31. Gupta, L. et al. Inflammation in cardiovascular disease: A comprehensive review of biomarkers and therapeutic targets. *Cureus* **15**, e45483 (2023).
32. Wu, J. et al. Lipidomic signatures align with inflammatory patterns and outcomes in critical illness. *Nat. Commun.* **13**, 6789 (2022).
33. Sung, Y. J. et al. Deep vein thrombosis exhibits characteristic serum and vein wall metabolic phenotypes in the inferior vena cava ligation mouse model. *Eur. J. Vasc. Endovasc.* **55**, 703–713 (2018).
34. Ma, N., et al. Plasma metabonomics and proteomics studies on the anti-thrombosis mechanism of aspirin eugenol ester in rat tail thrombosis model. *J. Proteom.* **215**, 103631 (2020).
35. Lee, T. Y. et al. Platelet autophagic machinery involved in thrombosis through a novel linkage of AMPK-MTOR to sphingolipid metabolism. *Autophagy* **17**, 4141–4158 (2021).
36. Engelmann, B. & Massberg, S. Thrombosis as an intravascular effector of innate immunity. *Nat. Rev. Immunol.* **13**, 34–45 (2013).
37. Byrnes, J. R. & Wolberg, A. S. Red blood cells in thrombosis. *Blood* **130**, 1795–1799 (2017).
38. Michno, A., Raszeja-Specht, A., Jankowska-Kulawy, A., Pawelczyk, T. & Szutowicz, A. Effect of L-carnitine on acetyl-CoA content and activity of blood platelets in healthy and diabetic persons. *Clin. Chem.* **51**, 1673–1682 (2005).
39. Hurot, J. M., Cucherat, M., Haugh, M. & Fouque, D. Effects of L-carnitine supplementation in maintenance Hemodialysis patients: A systematic review. *J. Am. Soc. Nephrol.* **13**, 708–714 (2002).
40. Maekawa, K. et al. Higher lactate and purine metabolite levels in erythrocyte-rich fresh venous thrombus: Potential markers for early deep vein thrombosis. *Thromb. Res.* **177**, 136–144 (2019).
41. Jiang, X. et al. Metabolites associated with the risk of incident venous thromboembolism: A metabolomic analysis. *J. Am. Heart Assoc.* **7**, e010317 (2018).
42. White, R. H. The epidemiology of venous thromboembolism. *Circulation* **107**, I4–I8 (2003).
43. Navarrete, S., et al. Pathophysiology of deep vein thrombosis. *Clin. Exp. Med.* **23**, 645–654 (2022).
44. Smith, C. A., Want, E. J., O'Maille, G., Abagyan, R. & Siuzdak, G. XCMS: Processing mass spectrometry data for metabolite profiling using Nonlinear peak alignment, matching, and identification. *Anal. Chem.* **78**, 779–787 (2006).
45. Gong, Y. et al. Metabolic-pathway-based subtyping of triple-negative breast cancer reveals potential therapeutic targets. *Cell Metab.* **33**, 51–64 (2021).
46. Liu, Q. et al. Altered faecal microbiome and metabolome in IgG4-related sclerosing cholangitis and primary sclerosing cholangitis. *Gut* **71**, 899–909 (2022).
47. Zhang, X. et al. Dietary cholesterol drives fatty liver-associated liver cancer by modulating gut microbiota and metabolites. *Gut* **70**, 761–774 (2021).
48. Xiao, Y., et al. Comprehensive metabolomics expands precision medicine for triple-negative breast cancer. *Cell Res.* **32**, 477–490 (2022).
49. Prakash, A. et al. Hybrid data acquisition and processing strategies with increased throughput and selectivity: pSMART Analysis for global qualitative and quantitative analysis. *J. Proteome Res.* **13**, 5415–5430 (2014).
50. Thevenot, E. A., Roux, A., Xu, Y., Ezan, E. & Junot, C. Analysis of the human adult urinary metabolome variations with age, body mass index, and gender by implementing a comprehensive workflow for univariate and OPLS statistical analyses. *J. Proteome Res.* **14**, 3322–3335 (2015).
51. Basu, S. et al. Sparse network modeling and metscape-based visualization methods for the analysis of large-scale metabolomics data. *Bioinformatics* **33**, 1545–1553 (2017).
52. Shannon, P. et al. Cytoscape: A software environment for integrated models of biomolecular interaction networks. *Genome Res.* **13**, 2498–2504 (2003).
53. Pang, Z. Q. et al. MetaboAnalyst 5.0: narrowing the gap between raw spectra and functional insights. *Nucleic Acids Res.* **49**, W388–W396 (2021).
54. Xia, J. G. & Wishart, D. S. MetPA: a web-based metabolomics tool for pathway analysis and visualization. *Bioinformatics* **26**, 2342–2344 (2010).
55. Jewison, T. et al. SMPDB 2.0: Big Improvements to the Small Molecule Pathway Database. *Nucleic Acids Res.* **42**, D478–D484 (2014).
56. Xia, J. G. & Wishart, D. S. MSEA: a web-based tool to identify biologically meaningful patterns in quantitative metabolomic data. *Nucleic Acids Res.* **38**, W71–W77 (2010).
57. Subramanian, A. et al. A next generation connectivity Map: L1000 platform and the first 1,000,000. *Profiles Cell* **171**, 1437–1452 e1417 (2017).
58. Franciosa, G. et al. Proteomics of resistance to Notch1 inhibition in acute lymphoblastic leukemia reveals targetable kinase signatures. *Nat. Commun.* **12**, 2507 (2021).
59. Members, C.-N. & Partners Database resources of the National Genomics Data Center, China National Center for Bioinformation in 2022. *Nucleic Acids Res.* **50**, D27–D38 (2022).
60. Chen, T. et al. The genome sequence archive family: Toward explosive data growth and diverse data types. *Genom. Proteom. Bioinform.* **19**, 578–583 (2021).
61. Ma, J. et al. iProX: an integrated proteome resource. *Nucleic Acids Res.* **47**, D1211–D1217 (2019).
62. Chen, T. et al. iProX in 2021: connecting proteomics data sharing with big data. *Nucleic Acids Res.* **50**, D1522–D1527 (2022).

Acknowledgements
We thank the dedicated participants who made this study possible. We thank the assistance from Shanghai Biotree Biotech Co.Ltd for plasma metabolomics analysis. We also thank the High-Performance Computing Platform and Instrument Analysis Center of Xi'an Jiaotong University for supporting this study. This study is supported by grants from the National Natural Science Foundation of China (32170616 (T.L.Y), 32370653 (Y.G), and 82170896 (Y.G)), Key Research and Development Project of Shaanxi Province (2019ZDLSF01-09 (H.Z.X) and 2022GXLH-01-22 (T.L.Y)), Social Development Foundation of Shaanxi Province (2022SF-394 (P.F.W)), Science Fund for Distinguished Young Scholars of Shaanxi Province (2021JC-02 (T.L.Y)), Innovation Capability Support Program of Shaanxi Province (2022TD-44 (T.L.Y)), Science and Technology Planning Project of Xi'an (2019115713YX012SF052 (K.Z)), and the Fundamental Research Funds for the Central Universities.

Author contributions
K.Z. performed the data analyses and wrote the manuscript. W. H., H.Z.X. and P.F.W. evaluated the clinical images and supervised sampling. S.H.T., H.W., J.B.C., Y.Z. (Yan Zou), Y.F.L., C.G.L. and D.Y.L. recruited samples and collected clinical data; Y.Z. (Ying Zhang) performed proteomics analyses. Y.R. generated figures for the manuscript. Y.G., K.Z. and T.L.Y. designed, coordinated, and supervised the project. Y.G., T.L.Y. and S.S.D. revised the manuscript. D.T. and N.Y. performed administrative assistance.

Competing interests
The authors declare no competing interests.

Additional information
Supplementary information The online version contains supplementary material available at https://doi.org/10.1038/s41467-024-52262-0.

Correspondence and requests for materials should be addressed to Kun Zhang, Tie-Lin Yang or Yan Guo.

Peer review information *Nature Communications* thanks Ahsan Khandoker, Antonino Tuttolomondo, Belinda Willard, and the other anonymous reviewer(s) for their contribution to the peer review of this work. A peer review file is available.